

# OPTIMAL THRESHOLDING TECHNIQUE FOR SHAPE AND SIZE DETECTION OF TARGET FROM THROUGH-THE-WALL RADAR IMAGE\*

---

---

### 4.1 Introduction

### 4.2 Methodology

#### *4.2.1 Data Acquisition*

#### *4.2.2 Average Subtraction*

#### *4.2.3 Image Formation*

#### *4.2.4 Image Enhancement*

#### *4.2.5 Formulation of Statistics Based Optimal Thresholding Technique and Implementation*

### 4.3 Results and Discussion

#### *4.3.1 Validation of Developed Thresholding Technique*

### 4.4 Conclusion

\*Part of this work has been published as:

**Akhilendra P. Singh**, Smrity Dwivedi, and Pradip K. Jain, "Development of optimal thresholding technique for shape and size detection for through-the-wall radar imaging system," *Defence Science Journal*, vol. 69, no. 6, pp. 531-626, 2019.



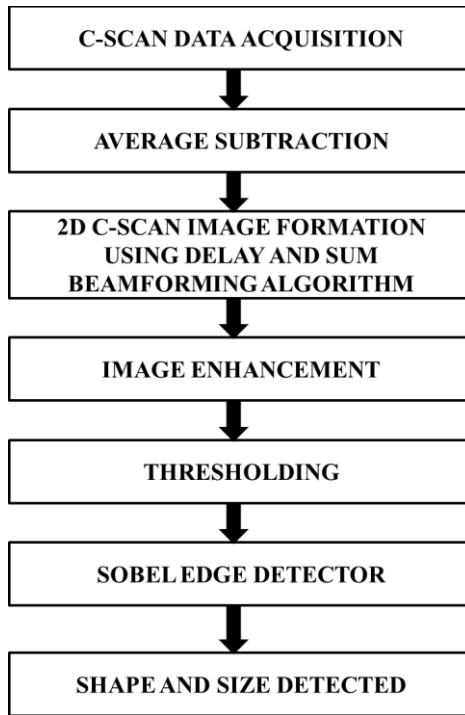
## 4.1 Introduction

The radar images show minimal resemblance to optical images due to which it becomes difficult to interpret from the imaged scene. The through-the-wall radar image of stationary targets behind a wall contain pixels reflected from the target as well as from the background noises or clutters. Therefore, it is required to separate the target pixels from the background noises or clutters in the image for recognition of the target. Hence, there is a need for a methodology that can automatically perform detection tasks and thereby help in decision making. The common aim of the detection method is to separate the target pixels from the background, thus eliminating the interference of background noises or clutters in the image. For this purpose, thresholding is applied to the image to separate target pixels from the background. Various researchers have reported about choosing an optimum threshold for mitigating background noises or clutters. Debes, Amin and Zoubir (2009) have used statistical detectors based on likelihood ratio tests for the detection of stationary targets in through-the-wall radar images. In this test, a Neyman-Pearson criterion was formulated for choosing a threshold for separating target pixels in through-the-wall radar images while controlling false alarm rate. However, this test has been requiring a priory probability density functions for the through-the-wall radar images. Since information about probability density functions is challenging to obtain a priory, therefore Debes *et al.* (2009a) have proposed a methodology that adapts the statistics parameters corresponds to the through-the-wall radar image statistics for implementation of the Neyman-Pearson test. Further, morphological filtering was used to optimize the estimates test parameters. These approaches provide quality images, but they assume a priory probability density functions of targets and clutters in radar images [Debes *et al.* (2010a)]. These assumed pdfs might

differ for the various scenarios. Therefore in most cases appropriate probability density functions and false alarm rate (FAR) need to define a priory every time for both targets and clutter in through-the-wall radar image, which presents a shortcoming of using these approaches for detection of the target. To overcome this shortcoming, some alternative automatic threshold selection techniques from the histogram of through-the-wall radar image have been proposed [Seng *et al.* (2013)]. Such techniques use a discriminant criterion by maximizing the separability of the resultant classes in order to select an optimal threshold. However, in most of the real scenarios, histograms of through-the-wall radar images do not exhibit a traceable valley. Therefore it becomes difficult to obtain an optimal threshold. Thus for mitigating background noises or clutters, various authors have reported their work in this field, but any concrete result has not been reported so far. Hence, there is a need for an optimal methodology to mitigate background noises or clutters in through-the-wall radar images for achieving a high-quality image representing the target position, shape, and size. Till now, it is challenging to achieve shape detection of the target from the through-the-wall radar system. In place of these approaches, an optimal algorithm/methodology has proposed for enhancement of detection of a target using curve fitting and genetic algorithm. In the proposed methodology, the fitness function will generate the optimized threshold value based on image statistics of the through-the-wall radar image of the target while controlling accuracy and false alarm in a user-defined constraint. The advantage of the proposed method is that it will not require the assumption of pdf and histogram in each scenario for choosing the optimum threshold.

## 4.2 Methodology

The developed methodology consists of data acquisition, average subtraction, 2D C-Scan through-the-wall image formation, image enhancement, and target detection. Flowchart of different steps applied is shown in Figure 4.1, and the detail of each step is discussed below.



**Figure 4.1.** Flowchart of methodology for detection of target shape and size.

#### **4.2.1 Data Acquisition**

For the development of optimal thresholding technique for shape and size detection of the target, an experiment has been carried out. C-scan data is collected using measurement set-up shown in Chapter 2 for different shapes and sizes of wooden and metallic targets having target id T1-T10. The details about list of the target is given in Table 4.1.

### 4.2.2 Average Subtraction

The received signal contains reflected signals from the target as wells as undesired signals. These undesired signals appears due to reflection from antenna mismatch and background noise. To mitigate these undesired signals, the average subtraction method is applied as proposed by Chandra *et al.* (2008). For this purpose, the mean vector of each B-scan is calculated and further subtracted from its each individual A-scan [Chandra *et al.* (2008)]

$$B_{ij} = A_{ij} - \left( \frac{1}{21} \sum_{j=1}^{21} A_{ij} \right) \quad (4.1)$$

where,  $i = 1, 2, \dots, 21$  (number of B-scans),  $j = 1, 2, \dots, 21$  (number of A-scans).

**Table 4.1.** Details about list of target samples considered

S. No.	Target I/D	Shape	Size	Orientation	Material
1	T1	square	30cmX30cm	0	metal
2	T2	square	35cmX35cm	0	metal
3	T3	square	30cmX30cm	0	wood
4	T4	rectangle	50cmX30cm	0	wood
5	T5	square	35cmX35cm	0	wood
6	T6	rectangle	55cmX35cm	0	metal
7	T7	circle	Dia=30cm	0	wood
8	T8	circle	Dia=35cm	0	wood
9	T9	circle	Dia=30cm	0	metal
10	T10	circle	Dia=35cm	0	metal

### 4.2.3 Image Formation


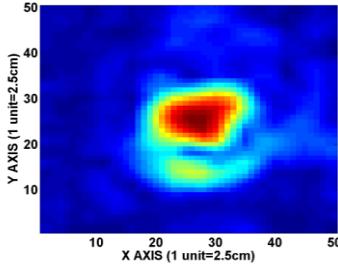

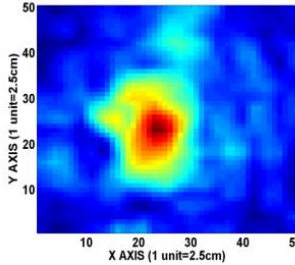
After performing average subtraction on acquired C-scan data, delay and sum beamforming algorithm is applied on C-scan data to form the through-the-wall radar images. The whole image map is divided into small pixels. For each pixel in the desired image map, the propagation delay from the one scan point to the pixel and then back to the same scan point is calculated. The details about the calculation of propagation delay can be

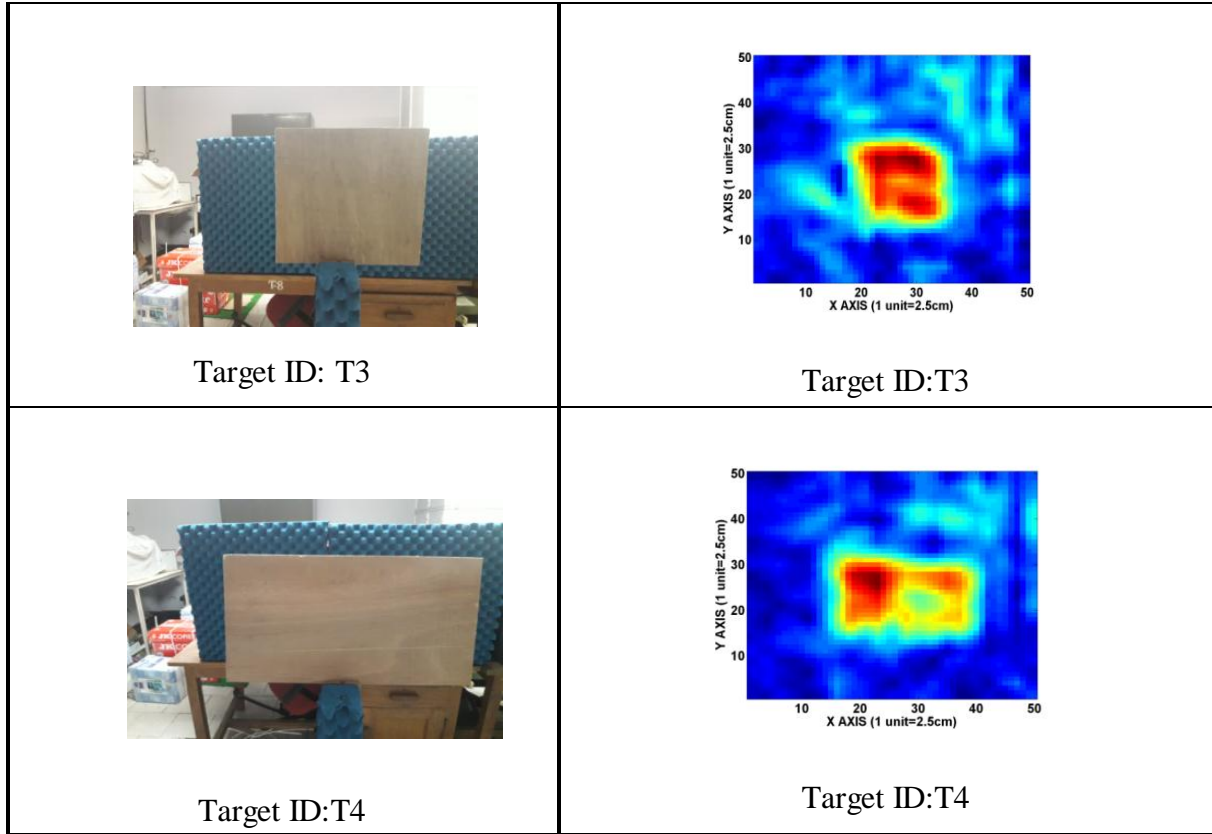
found in Chapter 3 [Ahmad *et al.* (2008)]. The value of each pixel is obtained using equation (3.16) which is given by [Ahmad *et al.* (2008)]

$$I(x_{p_i}, y_{p_i}, z_{p_i}) = \sum_{x_t=1}^{21} \sum_{y_t=1}^{21} \sum_{k=1}^{201} \sum_{i=1}^P S_{11}(x_t, y_t, f_m) \exp(j 2\pi f_k \tau_{p_i}) \quad (4.2)$$

Then, the two-dimensional C-Scan through-the-wall radar image of the target (horizontal cross-range vertical cross-range) is obtained by considering an XY plane at a fixed target range bin ( $z = z_{target}$ ), which is selected by observing the range profile. Thus, a virtual image of size 50X50 pixels has formed. The 2D C-Scan through-the-wall radar image (crossrange vs height) of the metallic square (Target id-T1), metallic square (Target id-T2), wooden square (Target id-T3), and wooden rectangle (Target id-T4), target at 0-degree rotation with its actual target shape is shown in Table 4.2.

**Table 4.2.** 2D C-Scan through-the-wall radar image obtained using delay and sum beamforming method on imaging plane along X and Y axis with its actual shape of target id (a) T1, (b) T2, (c) T3 and (d) T4.

Actual Shape of Target	2D C-scan through-the-wall radar image
 <p data-bbox="451 1503 586 1535">Target T1</p>	 <p data-bbox="1052 1503 1187 1535">Target T1</p>
 <p data-bbox="431 1856 613 1887">Target ID: T2</p>	 <p data-bbox="1031 1866 1213 1898">Target ID: T2</p>



#### 4.2.4 Image Enhancement

The 2D C-scan through-the-wall radar image may contain unwanted pixels, other than desired target pixels, due to background noise. Therefore, for enhancement of target pixels, various image enhancement methods such as spatial maximum filtering, mean filtering, Wiener filtering, and adaptive median filtering are considered for investigation [Gonzalez and Woods (2007)]. Peak to Signal Noise Ratio (PSNR) is calculated to compare their performance of filtering operation. PSNR is calculated from a 2D C-scan image and filtered image according to equations (4.3) and (4.4) [Verma *et al.* (2009)]

$$\text{Mean Square Error (MSE)} = \frac{1}{UXV} \sum_{i=1}^V \sum_{j=1}^U (E(i, j) - I(i, j))^2 \quad (4.3)$$



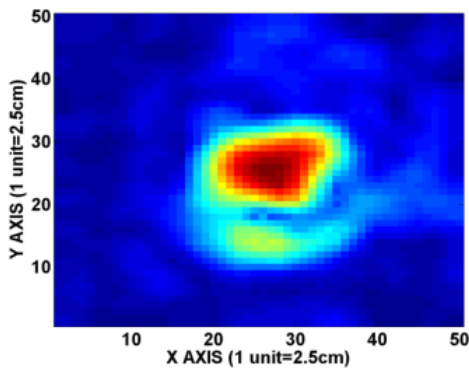
$$PSNR (dB) = 10\log\left(\frac{1}{MSE}\right) \quad (4.4)$$

where  $I$  represent a 2D C-scan through-the-wall radar image,  $E$  represent a 2D C-Scan through-the-wall radar after applying spatial filtering,  $U$  represents no of pixels in row, and  $V$  represents number of pixels in the columns.

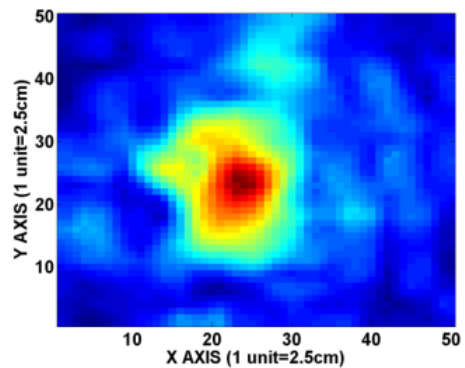
**Table 4.3.** PSNR (dB) value of enhanced 2D C-scan through-the-wall radar image of targets T1, T2, T3, and T4 after applying various spatial filtering techniques

Filtering method	T1	T2	T3	T4
Spatial max	25.15	24.55	24.04	24.75
Mean	39.05	38.86	33.56	33.86
Weiner	41.9	42.08	36.56	37.28
Adaptive median	47.22	50.09	42.07	44.47

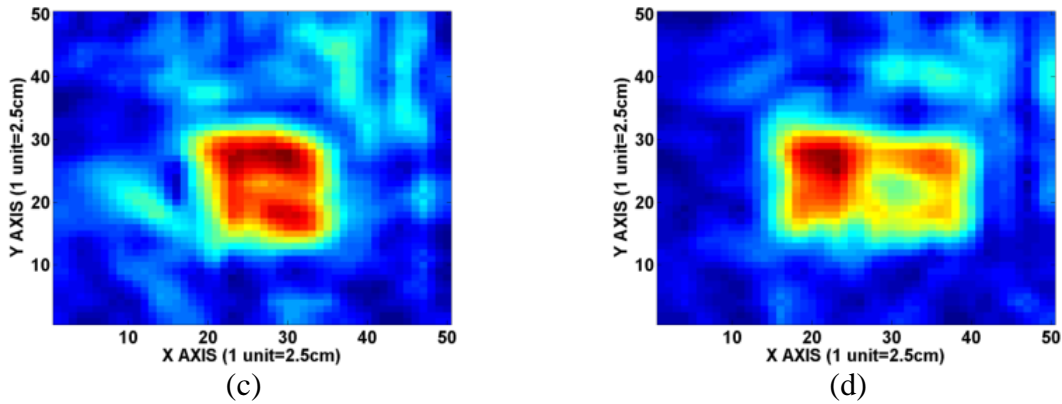
As shown in Table 4.3, the PSNR value of the adaptive median filter is higher compare to spatial filtering techniques. This shows that the adaptive median filter gives good results in comparison with other filtering operations. The adaptive median filtered image of considered targets is shown in Figs. 4.2a, 4.2b, 4.2c and 4.2d. These enhanced images are further used for process of detection.



(a)



(b)



**Figure 4.2.** Adaptive median filtered image of targets (a) T1, (b) T2, (c) T3, and (d) T4.

#### 4.2.5. Formulation of Statistics Based Optimal Thresholding Technique and

##### *Implementation*

From the through-the-wall radar image (TWRI) of the considered targets, it is observed that reflection from different shape and sizes of wooden and metallic targets have different levels of intensity. For detecting these targets, a proper threshold has to be chosen carefully. Therefore, statistics based thresholding technique is proposed to detect the shape and size of targets. The statistics based threshold is defined as

$$Th = \mu + n \times \sigma \quad (4.5)$$

Here “n” is called a scaling parameter. The image statistics may differ for two 2D C-scan through-the-wall radar images of a similar scenario therefore, a parameter ‘n’ is included to make equation adaptive in nature for thresholding.

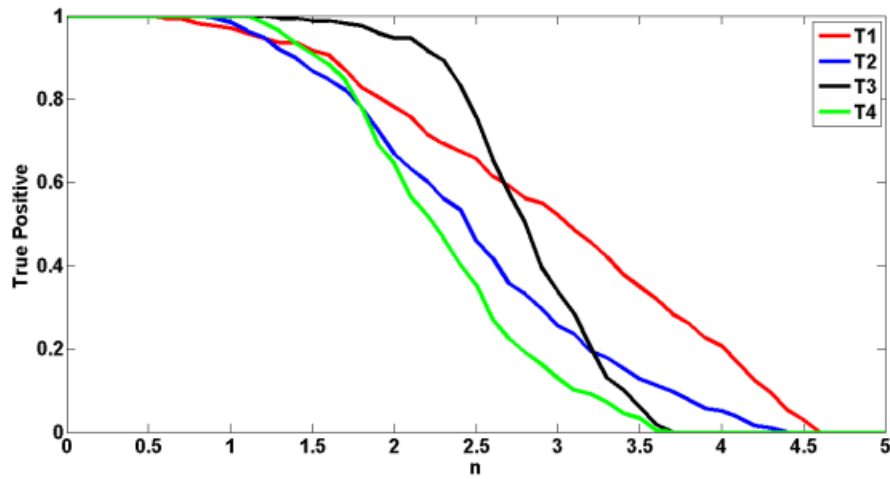
The statistics based thresholding technique should give such a threshold that would minimize the false detection of pixels for obtaining the accurate size. Therefore optimum of the value of ‘n’ is selected based on some parametric analysis so that the desired goal can be achieved. For this purpose, true positive (TP) and false positive (FP) values are computed from the 2D C-scan image of target using equations (4.6) and (4.7).

$$TP = \frac{\text{True detected target pixels}}{\text{Total no. of target pixels}} \quad (4.6)$$

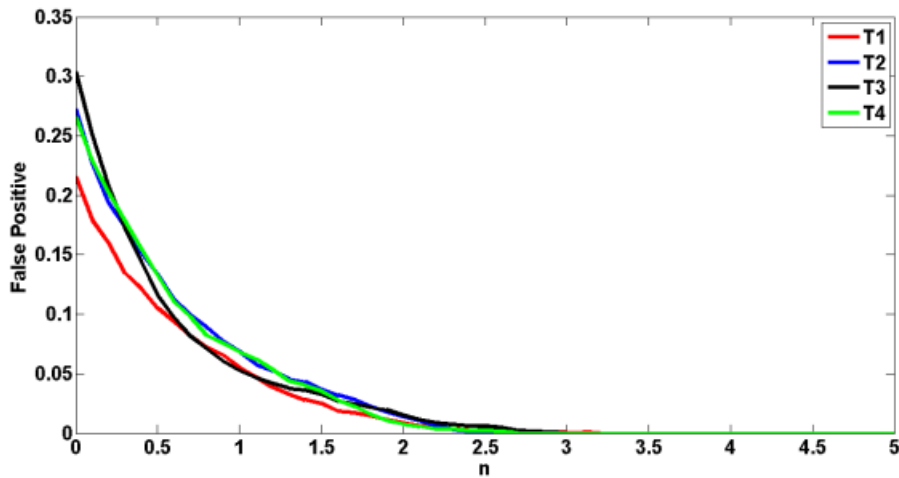
$$FP = \frac{\text{False detected target pixels}}{\text{Total pixels} - \text{Total no. of target pixels}} \quad (4.7)$$

The true positive value gives the accuracy of target pixels detected and false-positive value gives the false detected pixels. For the purpose of formulating a threshold criterion, 10 randomly selected targets T1-T10 is considered. The total number of pixels of each target is calculated using apriory information about target size, and pixel size of the image [Singh *et al.* (2009), Ibrahim *et al.* (2014), Kumar *et al.* (2017)]. For example, the sizes of target T1 and T3 are nearly equal to (30cm × 30cm) which covers approximate (12 × 12 = 144) pixels, the size of target T2 is nearly equal to (35cm × 35cm) which covers approximate (14 × 14) pixels and the size of T4 is nearly equal to (50cm×30cm) which covers approximate (20 × 12) pixels, respectively. Similarly the total number of pixels of each target has been calculated for other targets also. The boundary of targets region is defined using ground truth information about the location of the target and its size. The pixels detected inside the defined boundary of the target region are considered as true detected pixels. If the pixels are detected outside the defined boundary of the target region, then it denotes false detected pixels. The pixels not detected under the defined boundary of the target region denote missed pixels point.

The TP and FP values for Target ID T1-T10 are calculated for values of n in the range of 0 to 5. The plot of TP and FP value of a few of the considered targets T1, T2, T3, and T4 for different values of n is shown in Figures 4.3(a) and 4.3(b).



(a)



(b)

**Figure 4.3.** (a) Plot of True positive for different values of  $n$  of concealed targets having target id T1, T2, T3 and T4. (b) Plot of False positive for different values of  $n$  of concealed targets having target id T1, T2, T3 and T4.

It is observed that TP and FP value decreases with increasing the value of ' $n$ '. For a certain value of ' $n$ ', TP remains near the desired true positive value (i.e., 1). On the other side, the FP value also decreases as the value of ' $n$ ' increases. Hence, there is a need to find optimal value of  $n$  at which TP value is maximum and FP value is minimum. For this purpose, an empirical relation of TP and FP with scaling parameter ' $n$ ' is obtained using

curve-fitting . After analyzing several relations with ten test targets T1-T10, the following empirical relations are chosen whose coefficient of determination (R2) values found to be greater than 0.9 for both the relations.

$$TP(n) = a1 \exp \left( -0.6 \times \left( \frac{-(m+n*s-b1)}{c1} \right)^2 \right) \quad (4.8)$$

$$FP(n) = a2 \exp \left( -0.6 \times \left( \frac{-(m+n \times s-b2)}{c2} \right)^2 \right) \quad (4.9)$$

where m and s are the mean and standard deviation. The value of constants a1, b1, c1, a2, b2 and c2 for considered targets in equations (4.8) and (4.9) are given in Table 4.4.

**Table 4.4.** Constant value of TP and FP with its R2 for considered targets.

Target ID	a1	b1	c1	R2	a2	b2	c2	R2
T1	1.012	0.2786	0.3775	0.98	5.615	-0.8299	0.4162	99.8
T2	1.033	0.3416	0.2791	0.99	5.611	-0.8297	0.4161	99.8
T3	1.11	0.4673	0.2923	0.95	2369	-2.125	0.6142	99.2
T4	1.07	0.3921	0.2702	0.99	6.339	-0.8051	0.4535	99.7
T5	1.052	0.3708	0.328	0.98	3192	-2.497	0.6714	98.3
T6	0.9652	0.2505	0.3243	0.99	2506	-3.038	0.8121	98
T7	1.095	0.4388	-0.2917	0.95	3002	-1.917	0.5528	98.94
T8	1.03	0.3335	-0.3452	0.98	3225	-3.095	0.8235	92.7
T9	1.05	0.3443	0.3576	0.97	3409	-2.906	0.765	96.6
T10	1.028	0.2701	0.367	0.99	106	-1.209	0.4131	99.4
<i>Average</i>	<i>1.0445</i>	<i>0.3488</i>	<i>0.1959</i>		<i>1782.6</i>	<i>-1.92517</i>	<i>0.59379</i>	

After establishing the empirical relation of TP and FP with n, the next step is to find optimal value of n at which TP value is maximum and FP value is minimum. Such type of problem can be addressed using a multi-objective optimization problem. The value of constants a1, b1, c1, a2, b2 and c2 in equations (4.8) and (4.9) are replaced from their average values as shown in Table 4.4. For optimization, genetic algorithm (GA) is preferred. GA is an optimization technique that is globally used for large-scale optimization problems. We

preferred to use GA due to its interesting property such as efficiency, simple programmability and robustness.

To solve multiobjective optimization problem, the function  $Y(n)$  is divided into two vector functions of  $Y1(n)$  and  $Y2(n)$  and defines as

Minimizing  $Y(n) = [Y1(n), Y2(n)]$ ;  $0 < n < 5$  Such that  $Y1(n) = -TP(n)$  and  $Y2(n) = FP(n)$ .

The aim is to maximize  $TP(n)$  and minimize  $FP(n)$  and thereby find the optimum value of  $n$ . Thus the goal is to be set in such a manner that  $FP$  should be lesser than  $ub_{FP}$  and  $TP$  should be greater than the  $lb_{TP}$ . The goal vector is defined as

$$\text{Goal} = [-lb_{TP} \ ub_{FP}] \text{ for fitness function } Y(n) = [Y1(n), Y2(n)].$$

This will give the critical value of  $n$  for which  $TP > lb_{TP}$  and  $FP < ub_{FP}$ . Thus, the optimal threshold value can be obtained by putting the critical value of  $n$  in Equation (4.5).

### 4.3 Results and Discussion

The developed algorithm is tested with various targets. The following steps are performed for detecting the target using the developed algorithm.

Step 1: Mean and Standard deviation are calculated from the test image.

Step 2: The optimization goal for GA has been set as per the user requirement of  $TP$  and  $FP$ . Here,  $FP \leq 5\%$  and  $TP \geq 90\%$  is considered.

Step 3: The optimum value of  $n$  is computed with the help of GA optimization, using equations 6 and 7 within the constraint:  $0 < n < 5$ .

Step 4: Putting the optimum value of  $n$  in equation (4.5), the optimal threshold value is obtained.

The test results of the developed algorithm of various targets  $T1$ ,  $T2$ ,  $T3$ ,  $T4$  are shown in Table 4.5. The results show that the proposed methodology successfully detect targets

pixels with more than 90% accuracy and also achieved nearly less than 5% of false alarm, which was the desired aim of the proposed target detection algorithm. Furthermore, the performance of the proposed algorithm for target detection based on true positive (TP) and false positive (FP) value is compared with existing thresholding methods such as maximum entropy-based thresholding

**Table 4.5.** Comparison of thresholding techniques based on TP and FP for targets T1, T2, T3, T4.

S. No.	Thresholding methods	True Positive				False Positive			
		T1	T2	T3	T4	T1	T2	T3	T4
1	Otsu	0.83	0.81	0.99	0.91	0.01	0.03	0.04	0.03
2	Entropy	0.80	0.85	0.98	0.96	0.01	0.03	0.03	0.04
3	Mean	1	1	1	1	0.1	0.2	0.2	0.2
4	Statistical	0.95	0.95	1	0.98	0.04	0.05	0.04	0.05

method, mean iterative based thresholding method and Otsu's thresholding method [Wong and Sahoo (1989), Otsu (1979)]. Table 4.5 shows the TP and FP values using all four thresholding techniques for target Id T1, T2, T3, and T4. Otsu's method is a well-known global thresholding technique. This method gives a low false positive value for both metallic (Target id T3 and T4) and wooden target (Target id T1 and T2) but provides missed out pixel points for the wooden target (low dielectric targets). The maximum entropy-based thresholding method also gives a low false positive value for metallic targets but it gives missed pixels for the wooden target. Mean based iterative thresholding method provides true target detection for both metallic and wooden targets but it also provides a high false alarm. The proposed thresholding method provides true target detection and low false alarm for each class. It has observed that pre-existing thresholding methods give either false pixels or missed pixels. This occurs due to the wide variation in intensity among

targets. But proposed statistics-based thresholding method gives good results in comparison with other thresholding methods.

#### 4.3.1 Validation of Developed Thresholding Technique

The proposed algorithm has been designed to give a threshold value such that FP should be lesser than 5%, and TP should be greater than the lower boundary 90%. For validation of the developed algorithm, the proposed algorithm is tested with different through-the-wall radar images of targets which were earlier not used algorithm development and value of true pixel and the false pixel is computed. Figures 4.4(c), 4.4(d), 4.4(i), and 4.4(j) show the statistics based threshold image of targets T11, T12, T13 and T14 which are independent data samples and never used earlier for developing the algorithm. Table 4.7 shows the TP and FP values using the proposed adaptive statistical algorithm for the targets: T11, T12, T13, and T14. The value of the true pixel and the false pixel of test targets is shown in Table 4.7.

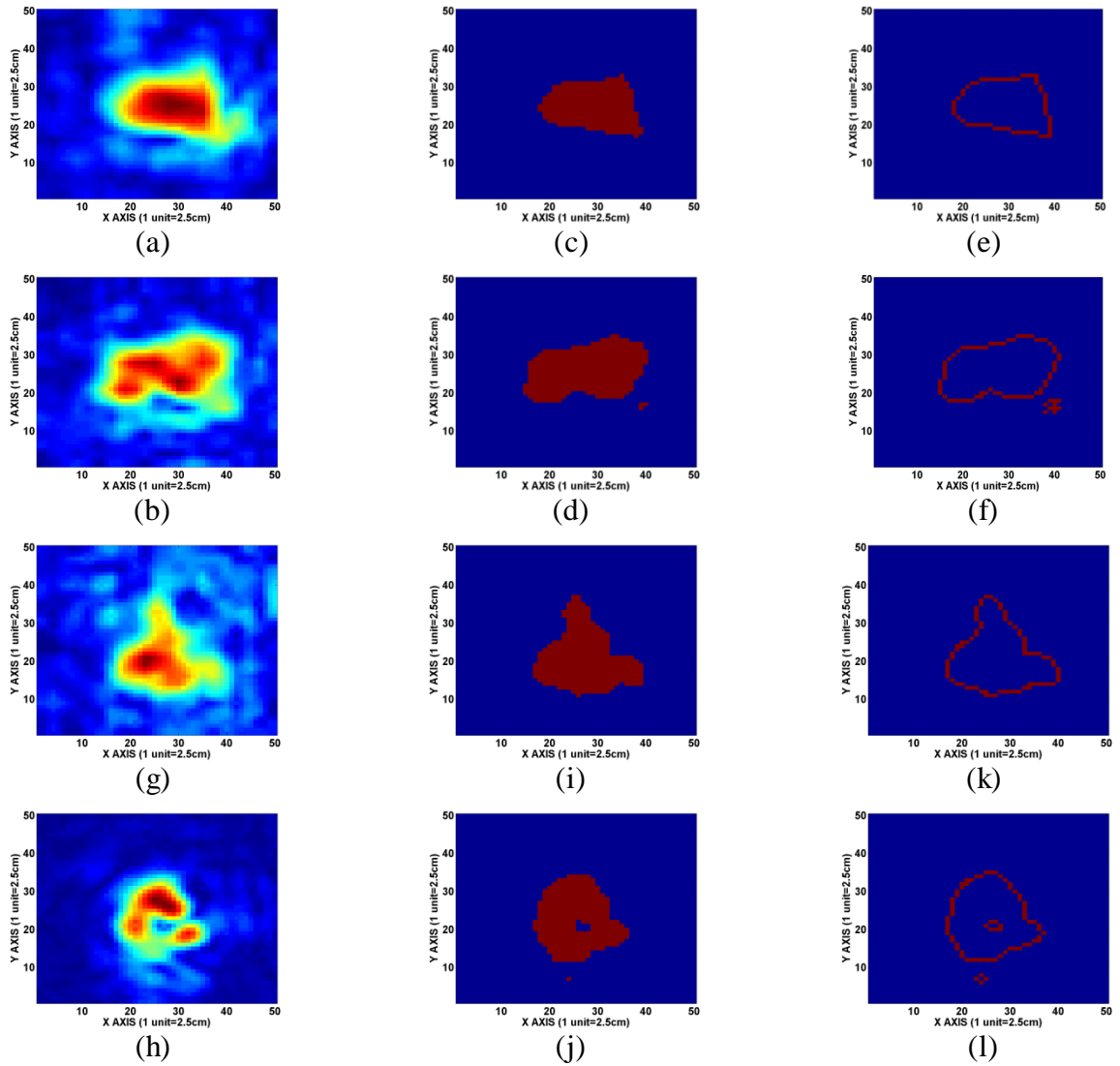
**Table 4.6.** Details about list of independent test target samples considered.

S. No.	Target I/D	Shape	Size (length X height)	Orientation	Material
11	T11	rectangle	50cmX30xm	0	metal
12	T12	rectangle	55cmX35cm	0	wood
13	T13	triangle	50cmX43cm	0	wood
14	T14	triangle	50cmX43cm	0	metal

**Table 4.7.** Values of scaling parameter “n” for targets T11, T12, T13 and T14 with TP and FP.

Target ID	Mean	Std	n	TP	FP
T11	0.2194	0.2230	1.4	1	0.09
T12	0.2338	0.2326	1.3	0.91	0.02
T13	0.2357	0.1817	1.1	0.92	0.03
T14	0.1830	0.2178	0.9	0.91	0.07





**Figure 4.4.** (a) 2D C-scan through-the-wall radar image of target T11. (b) 2D C-scan through-the-wall radar image of target T12. (c) 2D C-scan through-the-wall radar image of target T11 after applying proposed thresholding technique. (d) 2D C-scan through-the-wall radar image of target T12 after applying proposed thresholding technique. (e) 2D C-scan through-the-wall radar image of target T11 after applying Sobel edge detection. (f) 2D C-scan through-the-wall radar image of target T12 after applying Sobel edge detection. (g) 2D C-scan through-the-wall radar image of target T13. (h) 2D C-scan through-the-wall radar image of target T14. (i) 2D C-scan through-the-wall radar image of target T13 after applying proposed thresholding technique. (j) 2D C-scan through-the-wall radar image of target T14 after applying sobel edge detection. (k) 2D C-scan through-the-wall radar image of target T13 after applying Sobel edge detection. (l) 2D C-scan image of target T14 after applying Sobel edge detection.

The results show that the proposed algorithm detects target pixels with more than 90% accuracy, which was our desired aim of the proposed target detection methodology and also achieved nearly less than 5% of false alarm. The number of pixels detected in the target region for targets T11, T12, T13, and T14 are 245, 333, 321, and 306, respectively. This detection can provide vital information about the size of the target. After segmenting the target region from the background using thresholding, the shape of the target can be detected using an edge detection technique. Here, Sobel edge detection [Gonzalez and Woods (2009)] is used for shape detection of the target. The Sobel edge detector uses the first derivative and it is based on the gradient-based edge detector. After applying Sobel edge detection on the binary image of the target we were getting good accuracy in detection of the location of edge for all considered targets, so we preferred to use Sobel edge detection. Figures 4.4(e), 4.4(f), 4.4(k), and 4.4(l) show the detected shape of target T11, T12, T13, and T14 using Sobel edge detector. Thus it can be observed that the performance of the developed image statistics based detection algorithm for detection of target shape and size on different types of the target shows its adaptive nature.

#### **4.4 Conclusion**

In this chapter, an image statistics based adaptive thresholding technique for detection of target shape and size in 2D C-scan through-the-wall radar images has been formulated using curve fitting and genetic algorithm-based multi-objective optimization. The proposed target detection algorithm's capability was tested and validated with through-the-wall radar images of the wooden and metallic targets of different shapes and sizes. It has been found that based on the image statistics of the through-the-wall radar image of the

target, the fitness function provides an optimal threshold value while maintaining the user-defined constraints of accuracy and false alarm. The results showed that the proposed algorithm detects target pixels with more than 90% accuracy, which was our desired aim of the proposed target detection methodology and also achieved nearly less than 5% of false alarm. The good accuracy of the proposed algorithm shows that it can be implemented as a generalized.

